Hindawi Publishing Corporation
International Journal of Polymer Science
Volume 2013, Article ID 845432, 13 pages
http://dx.doi.org/10.1155/2013/845432

Research Article

Processing and Performance of Polymeric Transparent Conductive Composites

Parul Jain,[1] Ranjani Muralidharan,[1] Issac Sedloff,[1] Xiao Li,[1] Norma A. Alcantar,[2] and Julie P. Harmon[1]

[1] *Department of Chemistry, University of South Florida, 4202 East Fowler Avenue, CHE 205, Tampa, FL 33620-5250, USA*
[2] *Department of Chemical Engineering, University of South Florida, 4202 East Fowler Avenue, ENB 118, Tampa, FL 33620-5250, USA*

Correspondence should be addressed to Julie P. Harmon; harmon@usf.edu

Received 11 April 2013; Revised 18 June 2013; Accepted 27 June 2013

Academic Editor: Carmina Menchaca-Campos

Recent advances in microelectronic and optoelectronic industries have spurred interest in the development of reticulate doped polymer films containing "metallic" charge transfer complexes. In this study, such reticulate doped polymer films were prepared by exposing solid solutions of bis(ethylenedioxy) tetrathiafulvalene (BEDO-TTF) in polycarbonate (PC) to iodine, forming conductive charge transfer complexes. The resulting films exhibited room temperature conductivities ranging from 6.33 to 90.4×10^{-5} S · cm^{-1}. The colored iodine complexes in the film were reduced by cyclic voltammetry yielding conductive, colorless, transparent films. We were intrigued to examine the dielectric properties of BEDO-TTF in solid solution in PC prior to formation of the charge transfer complex as no such studies appear in the literature. Dielectric analysis (DEA) was used to probe relaxations in neat PC and BEDO-TTF/PC. BEDO-TTF plasticized the PC and decreased the glass transition temperature. Two secondary relaxations appeared in PC films, whereas the transitions merged in the BEDO-TTF/PC film. DEA also evidenced conductivity relaxations above 180°C which are characterized via electric modulus formalism and revealed that BEDO-TTF increased AC conductivity in PC.

1. Introduction

In the last few decades, there has been growing interest in conductive polymers and composites due to an array of potential applications in biological and chemical sensors, separations, microelectronics circuit boards, biomedical, coatings, and optical displays [1–5]. The ability to prepare thin, flexible, transparent films is an asset in applications requiring nanostructuring and miniaturization [6]. Conductivity is a general property of metals, but some polymers in combination with organic charge moieties exhibit metallic behavior [7]. After the discovery of the first organic superconductor, $(TMTSeF)_2PF_6$, a growing number of organic charge transfer complexes and conductive salts have been investigated [8]. These salts exhibit a charge transfer between a donors and acceptors in the solid state; the donors and acceptors molecules form segregated stacked sheets of cations and anions, respectively [9–11]. These materials also have low critical temperatures, Tcs (the temperature below which material is superconducting). $(TMTSeF)_2PF_6$ was subsequently replaced by another class of organic superconductors with BEDT-TTF (bis(ethylenedithio)tetrathiafulvalene) donors (Figure 1(a)) containing sulfur heterocycles [9]. The peripheral sulfur atoms allow better orbital overlap between donor stacks, forming a two-dimensional network. Suzuki et al. proposed that the substitution of sulfur or selenium atoms by lighter atoms, such as oxygen, would increase the Tc of organic superconductors. They synthesized an oxygen analogue of BEDT-TTF, (bis(ethylenedioxy)tetrathiafulvalene) (BEDO-TTF) (Figure 1(b)) in which outer sulfur atoms are replaced by oxygen atoms [12, 13]. BEDO-TTF was synthesized postulating that π donation from oxygen atoms into tetrathiafulvalene ring would lower the first ionization energy and make it an easily oxidized donor molecule [14]. In its

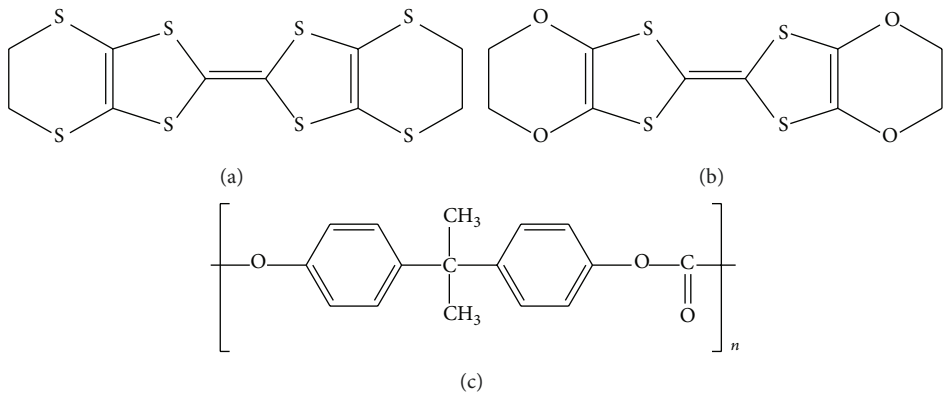

Figure 1: Molecular structure of (a) BEDT-TTF, (b) BEDO-TTF, and (c) polycarbonate.

partially oxidized state, the BEDO-TTF molecule has a tendency to self-aggregate via interactions in its peripheral heteroatoms. This results in the formation of a two-dimensional electronic structure, with metallic properties [15–19]. BEDO-TTF is of great interest in the design of organic superconductors, semiconductors, Langmuir-Blodgett films, crystalline organic metals, metal-like composites, biosensors, and soft electrodes [17, 20–23].

Surface conductive reticulate doped polymer (RDP) films are easily processed. The BEDO-TTF (donor) is an orange crystalline substance [13]. It is soluble in bisphenol A polycarbonate (PC) (Figure 1(c)) and easily processed into films. Bisphenol A polycarbonate, based on 2,2′-bis(4-hydroxyphenyl) propane, is a nonconductive amorphous polymer with optimum mechanical properties, optical properties, thermal stability, corrosion resistance, low density, and low cost [24, 25]. Jeszka and coworkers prepared films with BEDO-TTF/PC complexed with iodine and bromine to yield charge transfer complexes with conductive surfaces [26]. Both exhibited metallic properties; however, the Br doped films were clear, while the iodine films were dark colored and did not transmit light. Additionally, BEDO-TTF/PC iodine films were metallic down to 10 K, whereas BEDO-TTF/PC bromine films were metallic to about 100 K. Both of these films exhibited surface conductivity higher than 10^{-3} S/sq [26]. Work by all of these researchers spurred us to investigate reticulate doped PC films with BEDO-TTF/halogen charge transfer complexes for use in the construction of sensors designed to detect nitroaromatic compounds [27]. Hopefully, sensors can be designed to detect via changes in current specific to the type and concentration of the nitroaromatics detected. An additional desired property is transparency which has the potential of allowing any changes in spectroscopic properties that accompany binding of the nitroaromatics to be detected. This paper describes the processing of a series of RDP charge transfer complexes. It also reports on electrochemical methodology used to control the oxidation state of iodine species and to induce transparency in the BEDO-TTF/iodine films [28]. In the course of this investigation, we thought that it is important to further delve into the properties of BEDO-TTF dissolved in PC prior to complexation with halogens. We use dielectric spectroscopy to characterize the effect of BEDO-TTF on the relaxation behavior of PC as well as to characterize the conductive nature of BEDO-TTF in the PC matrix. To date, no DEA analysis has been undertaken on these interesting systems.

2. Materials and Methods

2.1. Materials. Poly (bisphenol-A carbonate) with molecular weight 45,000 was obtained from Arcos (Fair Lawn, NJ, USA). BEDO-TTF was purchased from Synchem OHG (Felsberg, Hesse, Germany). Methylene chloride (DCM), iodine and potassium iodide were purchased from Sigma-Aldrich (St. Louis, MO, USA). Double distilled water (18.2 MΩ·cm) was purified using cascada BIO-water system (Port Washington, NY, USA).

2.2. Purification of Polycarbonate Resin. PC resin was dissolved in DCM at room temperature, precipitated in methanol, and dried for 2-3 days under a vacuum.

2.3. Film Casting. PC and BEDO-TTF/PC films were prepared by solution casting 1 wt% PC in DCM. Neat PC and PC containing 2 wt% BEDO-TTF were dissolved in DCM. Solutions were stirred until dissolution was complete, cast on a glass surfaces, and evaporated at room temperature for 24 hours. The films were subsequently dried in a vacuum oven at 40°C for 72 hrs. The neat films obtained by this method were colorless and transparent, whereas BEDO-TTF/PC films were pink and transparent.

Surface conductive reticulate iodine doped BEDO-TTF/PC films were prepared by dissolving iodine in DCM and pouring the solution into a vial with a level rim. BEDO-TTF/PC films mounted on the glass slide were placed 5 mm above the solvent level. Iodine exposure resulted in oxidation of BEDO-TTF and formation of BEDO-TTF/PC-Iodine salts on the surface of films [26]. Optimum conditions were obtained by varying the exposure time and concentration of iodine to minimize surface resistivity. Depending on the exposure time and concentration, BEDO-TTF/PC films

exhibit color ranging from shiny purple to dark green. Light purple to olive green films with metallic sheen are conductive. The metallic sheen increased as the optimum conductivity was reached. BEDO-TTF/PC films exposed for a longer period of time to iodine vapors exhibited dull green to dark purple color with no metallic sheen, thereby resulting in nonconductive films. Long exposure time led to changes in the oxidation state of BEDO-TTF, resulting films with nonconductive surfaces [26].

2.4. Characterization

2.4.1. Differential Scanning Calorimetry. Calorimetric experiments were carried out using TA Instruments DSC 2920. The amount of sample used was about 5 mgs, and the heating rate was maintained at 10°C/min. Samples were scanned in the range from 25 to 300°C and were encapsulated in hermetically sealed aluminum pans under a nitrogen purge rate of 70–80 mL/min. Temperature calibrations were performed with indium as a standard. All data analysis was performed using the TA instruments universal analysis program, version 3.9A. Two scans were performed for films: the first scan erased thermal history, and the second scan was used to determine the glass transition temperature.

2.4.2. Dielectric Analysis. Note that dielectric analysis was conducted on neat PC and BEDO-TTF/PC films. The iodine complexes conduct electricity and are not suitable for DEA. Dielectric measurements were performed with the TA instruments DEA 2970 using single surface electrodes. The samples were heated to 225°C to embed the sample into the channels of the single surface and then cooled to −120°C with liquid nitrogen. A maximum force of 250 N was exerted on the samples to achieve a minimum spacing of 0.25 mm, which ensures good contact between the samples and the sensors. The experiments were performed with the temperature range from −120 to 225°C, with 4°C increments through a frequency range of 1 Hz to 100 kHz. A dry helium atmospheric purge of 500 mL/min was used to create an inert atmosphere. Capacitance and conductance were measured as a function of time, temperature, and frequency to obtain the dielectric constant or permittivity (ε'), dielectric loss (ε''), and loss tangent (tan = $\varepsilon''/\varepsilon'$).

2.4.3. UV-Vis Spectroscopy. UV-Vis films and solutions measurements were performed using a Perkin Elmer Lambda 40 UV-Vis-NIR double beam spectrophotometer with scan range from 190 nm to 800 nm. The UV-vis spectra of PC, BEDO-TTF, and BEDO-TTF/PC solutions in dichloromethane were recorded using quartz cell with 1 cm path length and dichloromethane as reference solution. PC and BEDO-TTF/PC and BEDO-TTF/PC-Iodine doped films were scanned with quartz slide.

2.4.4. Optical Images. Surface morphology of the BEDO-TTF/PC-Iodine films was studied using a Leica optical microscope in the reflection mode.

2.4.5. Four-Point Probe. The four-point probe method was used for the resistivity measurements on BEDO-TTF/PC-Iodine films. The probe consists of four linearly arranged and equally spaced electrodes, which remain in contact with a sample. The current, I, was supplied to the material through two outside probes with the help of a Keithley 6221 DC and AC current source, and steady voltage across the other two inside probes, V, was determined by Keithley 6514 system electrometer. Resistivity of BEDO-TTF/PC-Iodine films was measured randomly at different locations on the film's surface. Voltages were measured in volts and current in milliampere. Electrical conductivity, σ, was obtained by simply inverting the corresponding values of the surface resistivity.

2.4.6. Electrochemistry. The electrochemical modifications on BEDO-TTF/PC-Iodine film (0.095 mol · L^{-1}, exposed for 2 minutes) were carried out using a CH 760 electrochemistry workstation (CH Instrument, TX, USA). An Ag/AgCl electrode (BASi) was used as the reference electrode, and a platinum wire was used as the counter electrode. The electrolyte was 0.1 M KI solution in water.

3. Results and Discussion

3.1. UV-Vis Spectroscopy. UV-vis spectra for solutions and films are shown in Figure 2. In solution, BEDO-TTF exhibits strong absorption peaks at 314 nm and 334 nm and a weaker absorption peak around 518 nm. These absorption bands have been observed in the molecular absorption of neutral BEDO-TTF (undoped) earlier [26]. PC in DCM exhibits an absorption peak at 235 nm and another at 265 nm with a shoulder around 271 nm. These absorptions are characteristic of the bisphenol A unit which exhibits a main absorbance band at 226 nm with a secondary band at 276 nm [29].

PC films with and without BEDO-TTF were scanned as well. The purpose was to note any scatter at wavelengths above the electronic transition bands. The films were approximately 50 microns thick. At this thickness the absorbance was over 3.0 at wavelengths below 390 nm. However, the baseline at wavelengths above the absorption maxima indicates a lack of any appreciable scattering, and this indicates that the BEDO-TTF did not fall out of solution in the PC matrix. BEDO-TTF/PC-Iodine doped films were not transparent and became more metallic in appearance as the conductivity increased.

3.2. Optical Images. Figure 3 shows surface morphology of BEDO-TTF/PC-Iodine films at different iodine concentrations, where the conductivity is maximum. The surface exhibits fine regular grooves on optimized BEDO-TTF/PC-Iodine films. Longer exposure times and lower iodine concentrations results yield more pronounced surface topology, which, as shown in the next section, correlates with increased conductivity.

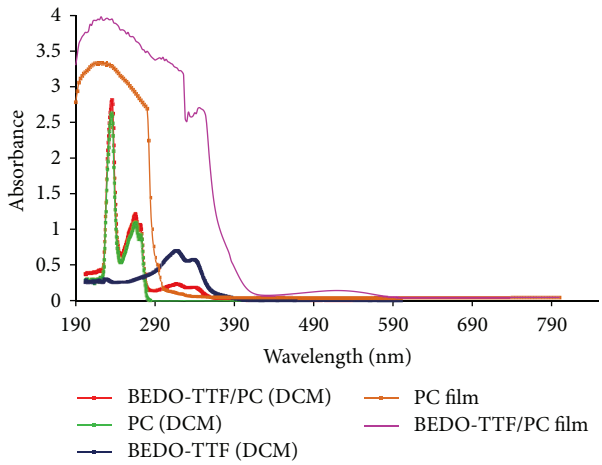

Figure 2: UV-Vis spectra of BEDO-TTF/PC,PC and BEDO-TTF dissolved in DCM and UV-Vis spectra of PC film and BEDO-TTF/PC film.

3.3. Electrical Properties

3.3.1. Four-Point Probe. Table 1 shows, as expected, that the surface of the BEDO-TTF/PC-Iodine films becomes conductive as a result of complex formation between acceptor iodine and donor species BEDO-TTF. This correlates with the surface topology viewed via light microscopy. The opposite side of the films are, of course, nonconductive [26]. It has been shown that there is a window of optimum exposure time, wherein the conductivity maximizes [26]. Beyond this time, films are nonconductive due to a change in the oxidation state of BEDO-TTF. Table 1 shows the calculated average resistivity and conductivity of these BEDO-TTF/PC-Iodine films. The exposure time required to reach minimum resistivity for each BEDO-TTF/PC-Iodine film increases with a decrease in iodine concentration. The surface resistivity values measured at three locations on the surface of the film were clustered closely around one central value. Standard deviations of surface resistivity for films when exposed for 2, 4, and 10 min are $\pm 1.0\,\text{K}\Omega/\text{sq}$, $\pm 0.02\,\text{K}\Omega/\text{sq}$, and $\pm 0.005\,\text{K}\Omega/\text{sq}$, respectively.

3.3.2. Electrochemical Properties. Figure 4 shows the cyclic voltammogram of BEDO-TTF/PC-Iodine film in 0.1 M KI solution. The oxidation peak at 0.5 V in the anodic scan corresponds to the oxidation of iodide to iodine, and the reduction peak at −0.15 V in the reverse scan is due to reduction of iodine to iodide [30, 31]. The oxidation and reduction of iodine at these potentials is also confirmed by the visual observation of the coloration of the film at high potentials and discoloration at low potentials. It is interesting to note that while the reversible oxidation/reduction peak of BEDO or TTF was reported ca. 0.4–0.6 V in organic solvents [14, 32], no distinguishable peak for BEDO-TTF was observed on the film in aqueous solution. This is due to the presence of iodine in the film which can react with BEDO-TTF [33]. Furthermore, the electrochemical method can be used to control the oxidation state of iodine species in the film. For instance, by holding the potential at −0.4 V, the iodine species in the film was reduced to iodide. Then, the conductivity of the reduced film was measured to ascertain the effect of iodine on the conductivity of the film. The discoloration gives rise to transparent film with 10% loss in conductivity. This finding encourages further studies on optimizing these systems.

3.3.3. Differential Scanning Calorimetry. The DSC thermograms for PC and BEDO-TTF/PC films are shown in Figure 5. The glass transition temperature for PC and BEDO-TTF/PC films are 148.5°C and 142.7°C, respectively [34–36]. The glass transition temperature of the BEDO-TTF/PC film decreased by about 6°C as compared to the neat film, indicating that the BEDO-TTF dissolves in and plasticizes the film.

3.3.4. Dielectric Analysis. The summary of dielectric analysis is provided for readers interested in a brief review. DEA is a thermal analysis technique well suited to the study of relaxations in polar polymers. In dielectric experiments, a sample is exposed to an alternating electric field, which generates an alternating electric polarization. The polarization causes the output current to lag behind the applied electric field by a phase shift angle, θ. DEA helps in determining the capacitance and conductance as $f(t,T,f)$ [37]. The capacitance and conductance of a material are measured over a range of temperatures and frequencies and are related to dielectric permittivity, ε', and dielectric loss factor, ε'', respectively. The dielectric permittivity, ε', represents the amount of dipole alignment (both induced and permanent), and the dielectric loss factor, ε'', measures the amount of energy required to align the dipoles or move ions. The complex permittivity, ε^*, is defined as follows [38]:

$$\begin{aligned} \varepsilon^* &= \varepsilon' - i\varepsilon'', \\ \varepsilon' &= \varepsilon'_{\text{induced dipole}} + \varepsilon'_{\text{alignment of dipole}}, \\ \varepsilon'' &= \varepsilon'_{\text{dipole loss factor}} + \varepsilon'_{\text{ionic conductance}}, \end{aligned} \tag{1}$$

where ε' and ε'' are the real and imaginary components of the dielectric complex permittivity ε^*. ε', dielectric constant or permittivity, represents the amount of dipole alignment both induced and permanent in the sample. The permittivity of a dielectric material is measured relative to that of a vacuum ($\varepsilon_o = 8.85 \times 10^{-1}\,\text{F}\cdot\text{m}^{-1}$) [39]. Plots of ε'' versus temperature maximize at temperatures that increase with frequency, f. Plots of $\ln f$ versus $1/T_{\max}$ are used to characterize transitions in polymers. Linear plots indicate secondary relaxations due to small scale motion such as side group rotation in the backbone. The large scale segmental motion accompanying the glass transition results in nonlinear plots discussed later.

However, at high temperatures conductivity often obscures the maxima noted in ε'' versus temperature. The Maxwell-Wagner-Sillars (MWS) effect created in a heterogeneous environment due to accumulation of charge, electrode polarization, impurities, and so forth masks relaxation behavior [40–43].

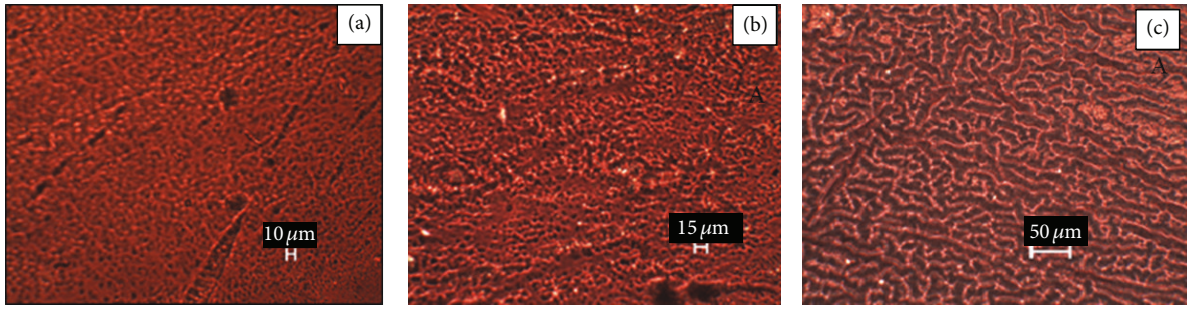

Figure 3: Optical images of BEDO-TTF/PC-Iodine film surface obtained using the transmission mode of a Leica microscope at (20X) with different exposure times and I_2 concentration (a) 0.095 mol/L-2 min, (b) 0.063 mol/L-4 min, and (c) 0.033 mol/L-10 min.

Table 1: Surface resistivity and conductivity of BEDO-TTF/PC-Iodine films.

BEDO-TTF (wt%) in PC	Iodine conc. in DCM (mol L^{-1})	Exposure time (mins)	Surface resistivity (KΩ/sq)	Conductivity (S cm^{-1})
2	0.095	2	15.82 ± 1.0	$6.33E-05$
2	0.063	4	1.47 ± 0.02	$6.80E-04$
2	0.033	10	1.10 ± 0.005	$9.04E-04$

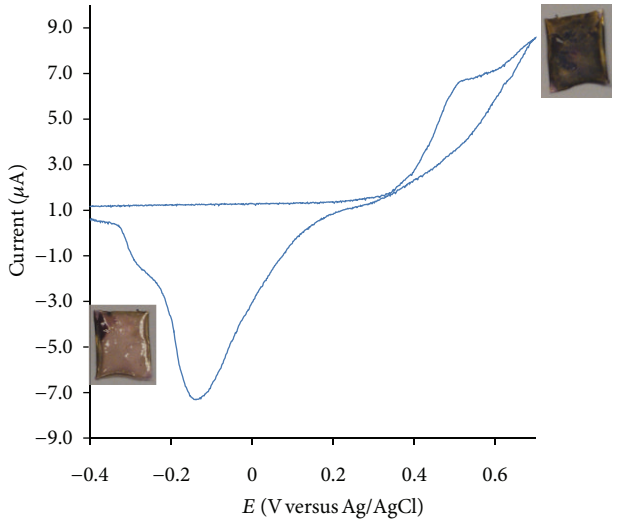

Figure 4: Cyclic voltammogram of BEDO-TTF/Iodine film with 0.095 mol/L (2 mins) in 0.1 M KI aqueous solution. Starting potential is 0.2 V, and scan rate is 5 mV/s.

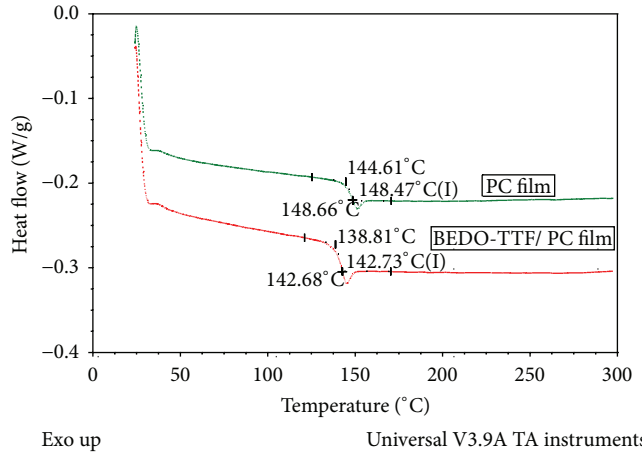

Figure 5: DSC thermograms for (a) PC film and (b) BEDO-TTF/PC film.

McCrum et al. formulated a mathematical treatment of the complex permittivity, ε^*, and defined electric modulus (M^*) as the inverse of the complex permittivity (ε^*) as follows [38]:

$$M^* = \frac{1}{\varepsilon^*} = M' + iM'' = \frac{\varepsilon'}{\varepsilon'^2 + \varepsilon''^2} + i\frac{\varepsilon''}{\varepsilon'^2 + \varepsilon''^2}, \quad (2)$$

where M^* is the complex electric modulus, M' is the electric storage modulus, and M'' is the electric loss modulus.

The dielectric loss spectra (ε'') versus temperature provide information on different relaxations, whereas loss modulus (M'') versus temperature reveal viscoelastic and ionic conductivity region. Figures 6(a) and 7(a) are plots of ε'' versus temperature for PC and BEDO-TTF/PC. Figures 6(b) and 7(b) are plots for M'' versus temperature for PC and BEDO-TTF/PC. The secondary β relaxation is enlarged in the insets of the ε'' plots. The glass transition region also exhibits clear maxima in ε'' versus temperature plots. Many other polymers exhibit conductivity effects that obscure the glass transition region. However, when electric modulus formalism is used, the glass transition region is again visible, but in addition, a high temperature relaxation, the conductivity relaxation, is noted. This region is important because it provides information for calculating AC and DC conductivities, as well as activation energies for ion translation [44]. Each relaxation region is further discussed in detail.

(1) *Secondary Relaxation*. The secondary relaxation, β, in PC has been widely studied by a host of techniques such as NMR [45–48], neutron scattering [49], molecular dynamic simulations [50], dynamic mechanical spectroscopy [51–54], dielectric analysis [55, 56], depolarized Rayleigh scattering

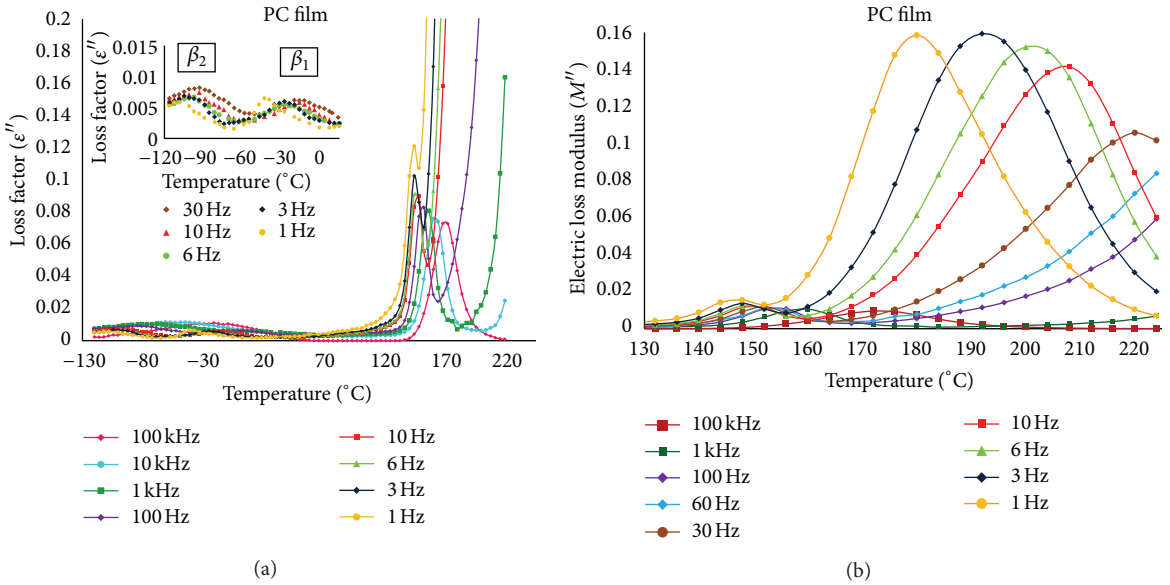

FIGURE 6: (a) ε'' versus temperature (°C) and (b) M'' versus temperature (°C) plots for PC film.

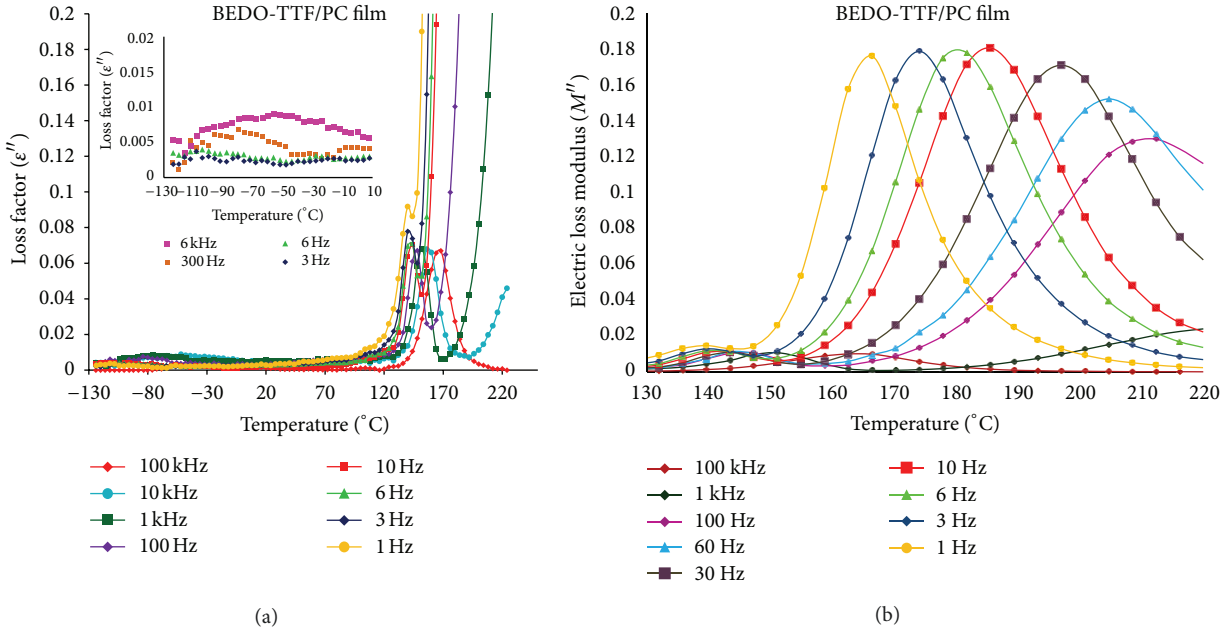

FIGURE 7: (a) ε'' versus temperature (°C) and (b) M'' versus temperature (°C) plots for BEDO-TTF/PC film.

[57], light scattering [58, 59], and thermally stimulated discharge current (TSC) [60]. Different explanations of the origin of beta relaxation have been proposed over the last few decades. Earlier investigations on PC ascertained that beta relaxation is a single, unresolved relaxation that involves rotation of carbonate groups [51, 55]. Later several studies were performed on beta relaxation over a broad frequency range and at the wide temperatures where the secondary transition separated into two or three regions resulting from phenyl ring motion, carbonate group motion, and coupled phenyl ring and carbonate motion [61–66]. Our DEA studies for PC reveal a broad β relaxation observed at higher frequencies (1 kHz–100 kHz). The inset in Figure 6(a) shows that the broad β relaxation process was further resolved prominently into two prominent components at lower frequencies (1 Hz–30 Hz). The relaxation occurring at higher temperature is termed as β_1 relaxation, whereas other peaks at lower temperatures are termed as β_2 relaxation. In comparison to PC, the BEDO-TTF/PC film exhibits only one secondary relaxation in the frequency range 1 Hz–100 kHz.

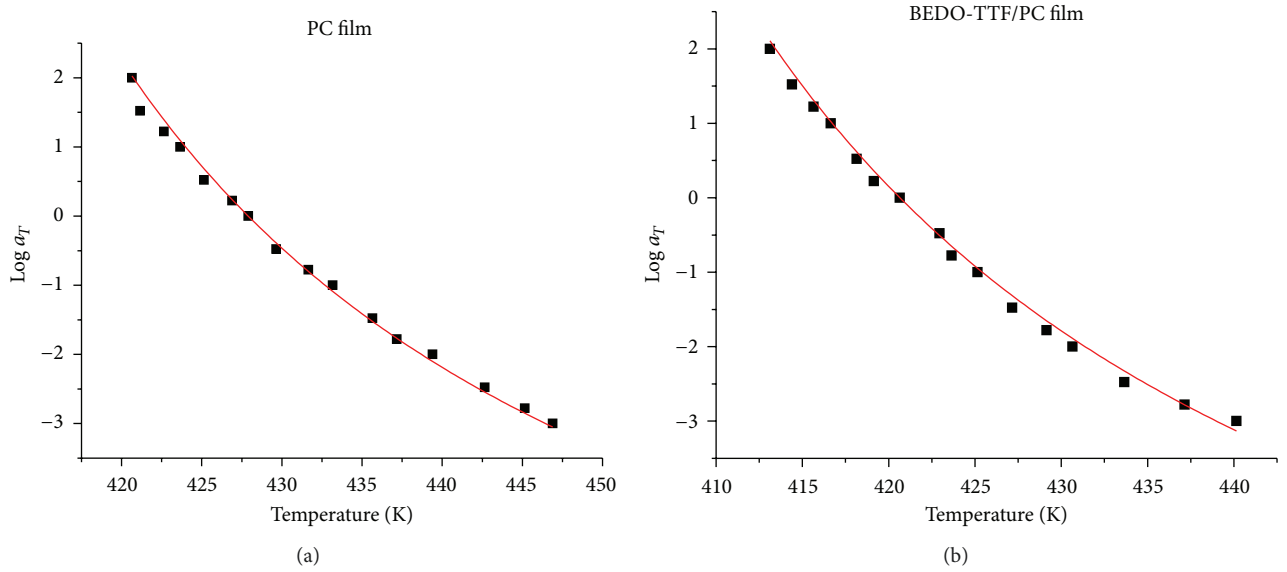

FIGURE 8: WLF plot for glass transition of (a) PC and (b) BEDO-TTF/PC films.

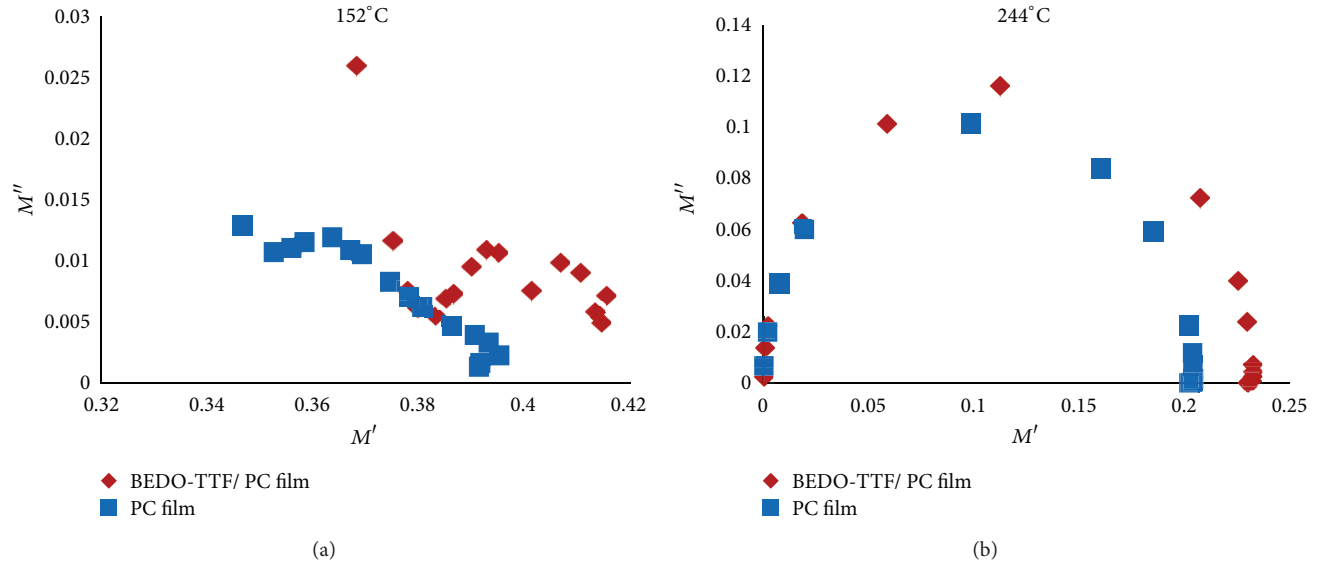

FIGURE 9: Argand plots derived from the conductivity relaxation region at different temperatures (152 and 224°C).

Peak maxima for each of the relaxation processes were assigned, and the slope of line obtained from Arrhenius plots of ln frequency versus reciprocal of temperature was used to calculate activation energies. The activation energies for β_1 and β_2 processes in PC in frequency range 1 Hz–30 Hz were found to be 44 and 54 kJ/mol, whereas for PC, it was determined to be 47 kJ/mole in frequency range 1 kHz–100 kHz. The activation energy for BEDO-TTF/PC in frequency range 1 kHz–100 kHz is 38 kJ/mole, respectively.

(2) *Primary Relaxation*. In PC, the alpha transition or glass transition involves micro-Brownian motion in the main chain and conformational changes in the phenyl groups [67, 68]. The α relaxation is discernible in ε'' versus temperature plots. The maxima in ε'' for Tg occur from 148 to 174°C for PC and from 140 to 168°C for BEDO-TTF/PC. The William-Landel-Ferry (WLF) equation (3) was used to characterized relaxation behavior [69, 70]. Plots of $\log a_T$ versus temperature were constructed as shown in Figure 8 Consider

$$\text{In } a_T = \log \frac{\tau(T)}{\tau(T_0)} = -\log \frac{\omega}{\omega_0} = \frac{-C_1(T - T_0)}{C_2 + (T - T_0)}, \quad (3)$$

where a_T is the shift factor that corresponds to frequency, T is a given temperature, T_0 is the reference temperature, τ is the relaxation time, and ω_0 is the angular frequency at

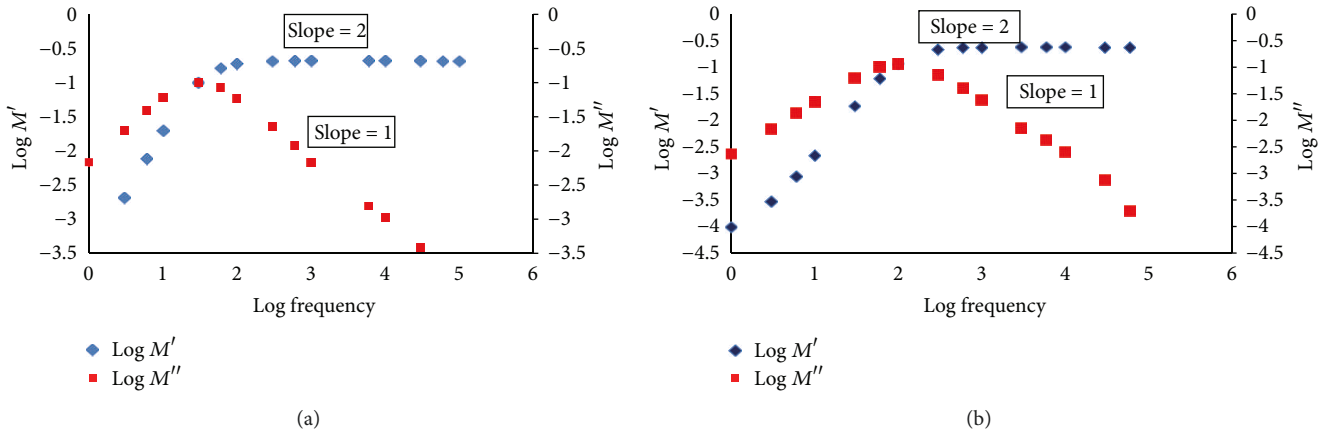

Figure 10: (a) Dependence of the real (M') and imaginary (M'') parts of the electric modulus on frequency in the region of the conductivity for PC and (b) BEDO-TTF/PC films, respectively.

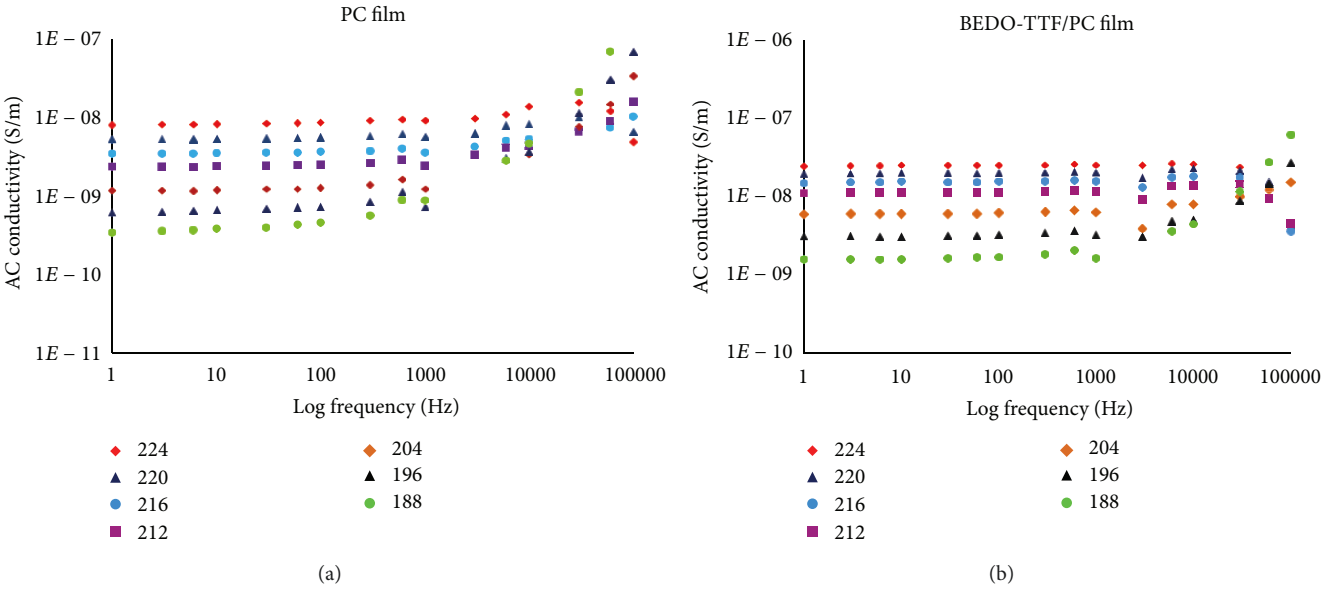

Figure 11: Frequency dependence of AC conductivity σ_{AC} (S/m) for (a) PC and (b) BEDO-TTF/PC film (2 wt%), respectively, above Tg temperature.

T_0. C_1, C_2, and T_0 are WLF constants that are determined by curve fitting the data to the WLF equation using Origin software as shown in Figures 8(a) and 8(b). The values of C_1, C_2, and T_0 were found to be 9.8, 42.7 K, and 427.9 K within a temperature range of 148–174°C for PC and 10.1, 43.8 K, and 420.6 K within a temperature range of 140–167°C for BEDO-TTF/PC, respectively. The WLF constants C_1 and C_2 reveal information related to fractional free volume (f_g) and thermal expansion (α_f) parameters through.

$$f_g = \frac{B}{(2.303 * C_1)}, \qquad \alpha_f = \frac{f_g}{C_2}, \tag{4}$$

where f_g is an unoccupied (free) volume in the structure and B is taken as unity according to Doolittle equation. The f_g for PC and BEDO-TTF/PC are 0.044 and 0.042, respectively, whereas the thermal expansion for PC and BEDO-TTF/PC is 1.03×10^{-3} and 0.958×10^{-3}, respectively. The apparent activation energy (ΔH) values for PC and BEDO-TTF/PC were calculated accordingly to the Catsiff and Tobolsky equation [71]:

$$\Delta H = 2.303 \left(\frac{C_1}{C_2}\right) R T_g^2. \tag{5}$$

The values of activation energies for PC and BEDO-TTF/PC films were found to be 813 kJ/mol and 785 kJ/mol, respectively. These values for PC are in the range of values of 480 and 835 kJ/mol as reported in the literature [45, 55, 72].

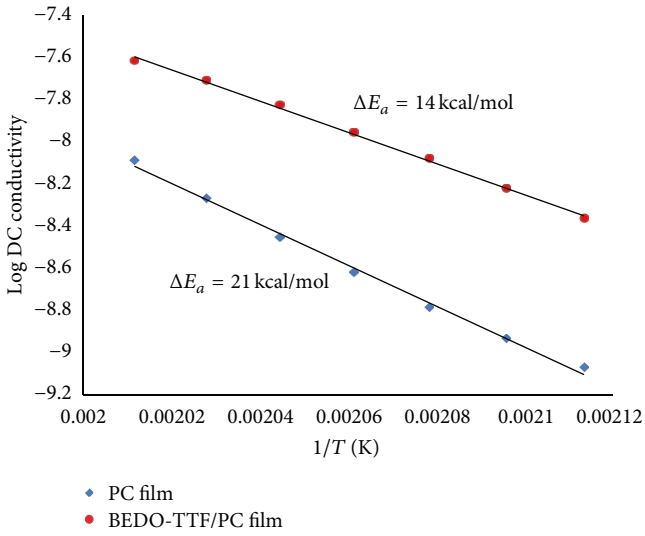

FIGURE 12: Log σ_{DC} versus inverse temperature plots of PC (red) and BEDO-TTF/PC film (blue).

WLF behavior for PC had been previously reported by others [39, 73–78].

Work herein demonstrates that BEDO-TTF plasticizes the PC matrix and reduces the glass transition temperature. Main chain motion occurs at lower temperatures in the BEDO-TTF plasticized film.

(3) *Ionic Conductivity Relaxation*. The high temperature region of the relaxation spectra was analyzed to confirm that the relaxation behavior was due to conductivity and not obstructed by any viscoelastic effects. Three proofs for this statement were undertaken, and these are described in the "the appendix" [28, 35]. This part of the research demonstrated that conductivity was enhanced in the PC containing BEDO-TTF, and this is likely a result of plasticization of the matrix.

4. Conclusion

This study first summarizes some of the excellent background work done by researchers in this field. The initial work reported herein reveals that films processed via the reticulate doped polymer method can be reduced by cyclic voltammetry to yield conductive, colorless, transparent films. These features make it possible to design optimum sensors. DSC studies of PC and BEDO-TTF/PC films reveal that the dye is soluble in and plasticized the PC matrix. Dielectric measurements carried out on PC and BEDO-TTF/PC confirm multiple transitions within the temperature range of −120 to 225°C for the frequency range 1–100 kHz. Different parameters such as relaxation broadening, activation energy, and conductivity (AC or DC) were found to be composition dependent. The AC conductivity becomes higher with the addition of BEDO-TTF. This is most likely due to enhanced mobility due to the plasticizing effect of the dye.

Appendix

*Proof (*Argand plot*).* The dielectric permittivity and loss factor for a relaxation with a single relaxation can be described by (A.1)

$$\varepsilon' = \varepsilon_U + \frac{(\varepsilon_R - \varepsilon_U)}{1 + \omega^2 \tau_E^2},$$
$$\varepsilon'' = (\varepsilon_R - \varepsilon_U) \frac{\omega \tau_E}{1 + \omega^2 \tau_E^2}, \tag{A.1}$$

where τ_E is the dielectric relaxation time and ω is the angular frequency. ε_U represents the high frequency, unrelaxed state, while ε_R represents the low frequency, relaxed state. By arranging (A.1), (A.2) is derived as

$$\left\{\varepsilon' - \frac{(\varepsilon_R - \varepsilon_U)}{2}\right\}^2 + (\varepsilon'')^2 = \left(\frac{\varepsilon_R - \varepsilon_U}{2}\right)^2. \tag{A.2}$$

Cole-Cole proposed that by plotting dielectric loss (ε'') against permittivity (ε') at a particular temperature, and a semicircle of radius $((\varepsilon_R - \varepsilon_U)/2)$ is obtained [38]. In Cole-Cole plots the high frequency region is on left side, while the low frequency exists on the right side of the plot. The Argand plots identify viscoelastic and conductivity effects [38, 79–81]. Argand plots were plotted between imaginary part (M'') of the complex modulus against real part (M') of the complex modulus as functions of the frequency at fixed temperatures. In an Argand plot, low frequency measurements exist on the left side of the semicircle, while the high frequency is on the right side. Argand plots can be obtained from

$$\left(M' - \left\{\frac{M_U - M_R}{2}\right\}\right)^2 + (M'')^2 = \left(\frac{(M_U - M_R)}{2}\right)^2. \tag{A.3}$$

Semicircular behavior is characteristic of Debye behavior for small rigid molecules and molecular liquids. This indicates a single relaxation time due to ionic conduction in the absence of any viscoelastic relaxation behavior [43]. By using the electric modulus, the space charge effects are reduced, and ionic conductivity peaks appear [82, 83]. Figure 9 shows semicircular behavior at 224°C. □

*Proof (*log M'', M' versus frequency*).* Ambrus et al. derived the electric modulus in terms of time, frequency, and modulus (see (A.4) and (A.5)) [84]. Starkweather et al. show that plots of log M'' and log M' versus log frequency at low frequencies will yield slopes of 1 and 2, respectively, when the electric modulus arises purely from ion conduction without contributions from viscoelastic relaxations [44]. Above Tg, the conduction is pure due to the diffusion of ions and independent of viscoelastic relaxation [14, 42, 81] as follows:

$$M = M_S \left(\frac{i\omega\tau_\sigma}{1 + i\omega\tau_\sigma}\right)$$
$$= M_s \left[\frac{(\omega\tau_\sigma)^2}{1 + (\omega\tau_\sigma)^2}\right] + iM_s \left[\frac{\omega\tau_\sigma}{1 + (\omega\tau_\sigma)^2}\right], \tag{A.4}$$

where

$$M_s = \frac{1}{\varepsilon_s}. \quad (A.5)$$

Figure 10 shows that above Tg, PC, and BEDO-TTF/PC films samples approach ideal value of 2 or 1, respectively, confirming ionic conductivity. □

*Proof (*AC and DC conductivities*).* When viscoelastic effects are negligible, the loss factor is described by (A.6). Upon rearrangement, AC conductivity can be obtained by (A.7)

$$\varepsilon'' = \frac{\sigma_{AC}}{\omega\varepsilon_0}, \quad (A.6)$$

where σ is the ionic conductivity, ω is the angular frequency ($2\pi f$), and ε_0 is the absolute permittivity of free space (8.854×10^{-14}) as follows:

$$\sigma_{AC} = \varepsilon''\omega\varepsilon_0. \quad (A.7)$$

As shown in Figures 11(a) and 11(b), the loss factor increases in the conductivity region at high temperatures and low frequencies.

Figure 11 shows frequency dependency of σ_{ac} at temperatures where conductivity effects dominate viscoelastic behavior. As temperature increases, σ_{ac} conductivity develops a plateau (ca.184°C) from 1 Hz to 10^2 Hz, signifying the beginning of the conductivity relaxation region. The σ_{ac} plateau then expands to higher frequencies 10^4 Hz as the temperature is increased, thus showing a frequency independent conductivity relaxation region. The absence of a frequency dependent region signifies negligible viscoelastic effects. This study reveals that the conductivity relaxation region exists between 180 and 224°C. At a lower temperature, where dielectric relaxation is dominant, the apparent conductivities (AC and DC) are strongly dependent on frequency. As temperature increases, conductivity becomes almost independent of the frequency. The BEDO-TTF/PC film has higher σ_{ac} values than that of the PC. The addition of BEDO-TTF presumably increases the amorphous content of the polymer. It speeds up segmental motion by increasing available free volume, thereby facilitating easy ion migration.

The DC conductivity values (σ_{DC}) have been obtained through the AC conductivity measurement [85–87] as shown by

$$\sigma_{AC}(\omega) = \omega\varepsilon_0\varepsilon''(\omega) = \sigma_{DC} + A\omega^s, \quad (A.8)$$

where ω is the angular frequency, ε_0 is the vaccum permittivity, ε'' is the imaginary part of the complex permittivity, A is the temperature dependent parameter, and s is the frequency dependent exponent of the "universal" power law. The exponent s lies between $0 \le S \le 1$ [81, 83]. Frequency independent AC conductivity has been observed at higher temperatures, which signifies the long-range movement of mobile charge carriers. At higher temperatures, the graph is seen as linear on a logarithmic scale. The plateau values give DC conductivity. The Arrhenius relationship is expressed by

$$\log\sigma_{DC} = \log\sigma_0 \exp\left(\frac{-E_A}{kT}\right), \quad (A.9)$$

where E_A is the apparent activation energy, σ_{DC} is the DC conductivity, σ_0 is the preexponential factor (conductivity at infinite temperature), and k is the Boltzmann constant.

Plots of In DC conductivity versus 1/temperature yield ionic conductivity and activation energies from the slopes. At higher temperatures, this plot exhibits a linear response. Figure 12 shows higher activation energy for PC (21 kcal/mole) due to lack of plasticization as compared to the plasticized BEDO-TTF/PC film which has activation energy of 14 kcal/mole. □

Conflict of Interests

None of the authors have conflict of interests with any of the aspects of this paper.

Acknowledgment

The authors would like to thank National Science Foundation for providing funding under Grant CBET 0808053 to support research.

References

[1] D. D. L. Chung, "Polymer-matrix composites for microelectronics," *Polymers and Polymer Composites*, vol. 8, no. 4, pp. 219–229, 2000.

[2] M. Gerard, A. Chaubey, and B. D. Malhotra, "Application of conducting polymers to biosensors," *Biosensors and Bioelectronics*, vol. 17, no. 5, pp. 345–359, 2002.

[3] B. W. Rowe, B. D. Freeman, and D. R. Paul, "Physical aging of ultrathin glassy polymer films tracked by gas permeability," *Polymer*, vol. 50, no. 23, pp. 5565–5575, 2009.

[4] C. M. Stafford, B. D. Vogt, C. Harrison, D. Julthongpiput, and R. Huang, "Elastic moduli of ultrathin amorphous polymer films," *Macromolecules*, vol. 39, no. 15, pp. 5095–5099, 2006.

[5] D. C. Wedge, A. Das, R. Dost et al., "Real-time vapour sensing using an OFET-based electronic nose and genetic programming," *Sensors and Actuators*, vol. 143, no. 1, pp. 365–372, 2009.

[6] C. Vree and S. G. Mayr, "Structure and surface morphology of vapor deposited polycarbonate thin films," *Journal of Applied Physics*, vol. 104, no. 8, Article ID 083517, 2008.

[7] J. K. Jeszka, A. Tracz, J. Ulanski, and M. Kryszewski, "Surface-conductive polymer films by reticulate doping with organic metals," *Journal of Physics D*, vol. 18, no. 10, pp. L167–L170, 1985.

[8] D. Jerome, A. Mazaud, M. Ribault, and K. Bechgaard, "Superconductivity in a synthetic organic conductor (TMTSF)2PF6," *Journal de Physique Lettres*, vol. 41, no. 4, pp. 95–98, 1980.

[9] T. Ishiguro, K. Yamaji, and G. Saito, *Organic Superconductors*, 2nd edition, 1998.

[10] R. P. Shibaeva, S. S. Khasanov, L. V. Zorina, and S. V. Simonov, "Structural features of low-dimensional molecular conductors: representatives of new hybrid polyfunctional materials: review," *Crystallography Reports*, vol. 51, no. 6, pp. 949–967, 2006.

[11] R. P. Shibaeva and E. B. Yagubskii, "Molecular conductors and superconductors based on trihalides of BEDT-TTF and some of its analogues," *Chemical Reviews*, vol. 104, no. 11, pp. 5347–5378, 2004.

[12] H. Kobayashi, A. Kobayashi, Y. Sasaki, G. Saito, and H. Inokuchi, "The crystal and molecular structures of bis(ethylenedithio)tetrathiafulvalene," *Bulletin of the Chemical Society of Japan*, vol. 59, no. 1, pp. 301–302, 1986.

[13] T. Suzuki, H. Yamochi, G. Srdanov, K. Hinkelmann, and F. Wudl, "Bis(ethylenedioxy)tetrathiafulvalene: the first oxygen-substituted tetrathiafulvalene," *Journal of the American Chemical Society*, vol. 111, no. 8, pp. 3108–3109, 1989.

[14] D. L. Lichtenberger, R. L. Johnston, K. Hinkelmann, T. Suzuki, and F. Wudl, "Relative electron donor strengths of tetrathiafulvene derivatives: effects of chemical substitutions and the molecular environment from a combined photoelectron and electrochemical study," *Journal of the American Chemical Society*, vol. 112, no. 9, pp. 3302–3307, 1990.

[15] M. A. Beno, H. H. Wang, A. M. Kini et al., "The first ambient pressure organic superconductor containing oxygen in the donor molecule, βm-(BEDO-TTF)3Cu2(NCS)3, Tc = 1.06 K," *Inorganic Chemistry*, vol. 29, no. 9, pp. 1599–1601, 1990.

[16] N. Drichko, R. Vlasova, V. Semkin et al., "Optical properties of a new organic metal $(BEDO\text{-}TTF)_5[CsHg(SCN)_4]_2$," *Synthetic Metals*, vol. 109, no. 1, pp. 123–127, 2000.

[17] S. Horiuchi, H. Yamochi, G. Saito, K.-I. Sakaguchi, and M. Kusunoki, "Nature and origin of stable metallic state in organic charge-transfer complexes of bis(ethylenedioxy)tetrathiafulvalene," *Journal of the American Chemical Society*, vol. 118, no. 36, pp. 8604–8622, 1996.

[18] H. Yamochi, T. Haneda, A. Tracz, and G. Saito, "Humidity dependent properties of a transparent conducting film doped with BEDO-TTF complex," *Physica Status Solidi*, vol. 249, no. 5, pp. 1012–1016, 2012.

[19] H. Yamochi, T. Nakamura, G. Saito et al., "The cation radical salts of the oxygen-substituted donor, BEDO-TTF," *Synthetic Metals*, vol. 42, no. 1-2, pp. 1741–1744, 1991.

[20] A. Graja, A. Brau, and J.-P. Farges, "Study of new conducting organic composites based on BEDO-TTF molecule," *Synthetic Metals*, vol. 122, no. 2, pp. 233–235, 2001.

[21] S. Horiuchi, H. Yamochi, G. Saito, and K. Matsumoto, "Structural and physical properties of molecular metals based on BEDO-TTF," *Synthetic Metals*, vol. 86, no. 1, pp. 1809–1810, 1997.

[22] H. Mochizuki, T. Mizokuro, N. Tanigaki, T. Hiraga, and I. Ueno, "Crystallization of bisphenol-A polycarbonate by a vacuum process," *Polymers for Advanced Technologies*, vol. 16, no. 1, pp. 67–69, 2005.

[23] H. Ohnuki, Y. Ishizaki, M. Suzuki et al., "Metallic Langmuir and Langmuir: blodgett films based on TTF derivatives and fatty acid," *Materials Science and Engineering C*, vol. 22, no. 2, pp. 227–232, 2002.

[24] S. C. Tjong and Y. Z. Meng, "Mechanical and thermal properties of polycarbonate composites reinforced with potassium titanate whiskers," *Journal of Applied Polymer Science*, vol. 72, no. 4, pp. 501–508, 1999.

[25] M. E. L. Wouters, D. P. Wolfs, M. C. van der Linde, J. H. P. Hovens, and A. H. A. Tinnemans, "Transparent UV curable antistatic hybrid coatings on polycarbonate prepared by the sol-gel method," *Progress in Organic Coatings*, vol. 51, no. 4, pp. 312–320, 2004.

[26] J. K. Jeszka, A. Tracz, A. Sroczyńska et al., "Metallic polymer composites with bis(ethylenedioxy)-tetrathiafulvalene salts. Preparation-properties relationship," *Synthetic Metals*, vol. 106, no. 2, pp. 75–83, 1999.

[27] N. A. Alcantar and J. Harmon, "Transparent conducting composites (TCCS) for creating chemically active surfaces," US Patent 8034302 B1, 2011.

[28] A. Tracz, J. K. Jeszka, A. Sroczynska et al., "New transparent, colorless, metallically conductive polymer films and their electrochemical transformations," *Synthetic Metals*, vol. 86, no. 1, pp. 2173–2174, 1997.

[29] A. Maroto, P. Kissingou, A. Diascorn et al., "Direct laser photo-induced fluorescence determination of bisphenol A," *Analytical and Bioanalytical Chemistry*, vol. 401, no. 9, pp. 3011–3017, 2011.

[30] P. H. Qi and J. B. Hiskey, "Electrochemical behavior of gold in iodide solutions," *Hydrometallurgy*, vol. 32, no. 2, pp. 161–179, 1993.

[31] Y. A. Yaraliyev, "Oxidation of iodide ions by means of cyclic voltammetry," *Electrochimica Acta*, vol. 29, no. 9, pp. 1213–1214, 1984.

[32] J.-P. Griffiths, R. J. Brown, P. Day, C. J. Matthews, B. Vital, and J. D. Wallis, "Synthesis of bis(ethylenedithio)tetrathiafulvalene derivatives with metal ion ligating centres," *Tetrahedron Letters*, vol. 44, no. 15, pp. 3127–3131, 2003.

[33] S. Horiuchi, H. Yamochi, G. Saito, and K. Matsumoto, "Highly-oxidized states of organic donor bis(ethylenedioxy)tetrathiafulvalene (BEDO-TTF)," *Molecular Crystals and Liquid Crystals Science and Technology*, vol. 284, pp. 357–365, 1996.

[34] M. D. Shelby and G. L. Wilkes, "Thermodynamic characterization of the oriented state of bisphenol A polycarbonate as it pertains to enhanced physical aging," *Journal of Polymer Science B*, vol. 36, no. 12, pp. 2111–2128, 1998.

[35] M. C. Delpech, F. M. B. Coutinho, and M. E. S. Habibe, "Bisphenol A-based polycarbonates: characterization of commercial samples," *Polymer Testing*, vol. 21, no. 2, pp. 155–161, 2002.

[36] J. Wang and Z. Xin, "Flame retardancy, thermal, rheological, and mechanical properties of polycarbonate/polysilsesquioxane system," *Journal of Applied Polymer Science*, vol. 115, no. 1, pp. 330–337, 2010.

[37] TA Instruments, DEA, 2790 dielectric analyzer, A - 057, TA instruments applications application library, http://www.tainst.com .

[38] N. G. McCrum, B. E. Read, and G. Williams, *Anelastic and Dielectric Effects in Polymeric Solids*, John Wiley and Sons, London, UK, 1967.

[39] J. P. Runt and J. J. Fitzgerald, *Dielectric Spectroscopy of Polymeric Materials: Fundamentals and Applications*, 1997.

[40] J. C. Maxwell, *Electricity and Magnetism*, vol. 1, Clarendon, Oxford, UK, 1892.

[41] K. W. Wagner, "Erklarung der dielectrischen nachwirkungsworgange auf grund maxwellscher vorstellungen," *Archiv Für Elektrotechnik*, vol. 2, pp. 371–387, 1914.

[42] R. W. Sillars, "The properties of a dielectric containing semiconducting particles of various shapes," *Journal of the Institution of Electrical Engineers*, vol. 80, no. 484, pp. 378–394, 1937.

[43] G. M. Tsangaris, G. C. Psarras, and N. Kouloumbi, "Electric modulus and interfacial polarization in composite polymeric systems," *Journal of Materials Science*, vol. 33, no. 8, pp. 2027–2037, 1998.

[44] H. W. Starkweather Jr. and P. Avakian, "Conductivity and the electric modulus in polymers," *Journal of Polymer Science B*, vol. 30, no. 6, pp. 637–641, 1992.

[45] S. Matsuoka and Y. Ishida, "Multiple transitions in polycarbonates," *Journal of Polymer Science, Polymer Symposia*, vol. 14, pp. 247–259, 1966.

[46] L. J. Garfield, "Molecular motions in some polycarbonates," *Journal of Polymer Science*, no. 30, pp. 551–559, 1970.

[47] D. Stefan and H. L. Williams, "Molecular motions in bisphenol A polycarbonates as measured by pulsed NMR techniques. I. Homopolymers and copolymers," *Journal of Applied Polymer Science*, vol. 18, no. 5, pp. 1279–1293, 1974.

[48] M. Wehrle, G. P. Hellmann, and H. W. Spiess, "Phenylene motion in polycarbonate and polycarbonate/additive mixtures," *Colloid & Polymer Science*, vol. 265, no. 9, pp. 815–822, 1987.

[49] S. Arrese-Igor, A. Arbe, A. Alegría, J. Colmenero, and B. Frick, "Secondary relaxation in two engineering thermoplastics by neutron scattering and dielectric spectroscopy," *Applied Physics A*, vol. 74, no. I, pp. S454–S456, 2002.

[50] J. H. Shih and C. L. Chen, "Molecular dynamics simulation of bisphenol A polycarbonate," *Macromolecules*, vol. 28, no. 13, pp. 4509–4515, 1995.

[51] F. P. Reding, J. A. Faucher, and R. D. Whitman, "Mechanical behavior of polycarbonates," *Journal of Polymer Science*, vol. 54, pp. S56–S58, 1961.

[52] C. I. Chung and J. A. Sauer, "Low-temperature mechanical relaxations in polymers containing aromatic groups," *Journal of Polymer Science*, vol. 9, no. 6, pp. 1097–1115, 1971.

[53] K. Varadarajan and R. F. Boyer, "Effects of thermal history, crystallinity, and solvent on the transitions, and relaxations in poly(bisphenol-A carbonate)," *Journal of Polymer Science*, vol. 20, no. 1, pp. 141–154, 1982.

[54] J. Y. Jho and A. F. Yee, "Secondary relaxation motion in bisphenol a polycarbonate," *Macromolecules*, vol. 24, no. 8, pp. 1905–1913, 1991.

[55] F. H. Muller and K. Huff, "Changes in the dielectric relaxation spectrum of high polymers on pulling and pretreatment," *Kolloid-Zeitschrift*, vol. 164, pp. 34–37, 1959.

[56] E. Sacher, "The contribution of the linear viscoelastic region to the impact properties of thin polymer films," *The American Chemical Society, Division of Organic Coatings and Plastics Chemistry*, vol. 34, no. 2, pp. 257–260, 1974.

[57] B. Erman, D. Wu, P. A. Irvine, D. C. Marvin, and P. J. Flory, "Optical anisotropy of the polycarbonate of diphenylolpropane," *Macromolecules*, vol. 15, no. 2, pp. 670–673, 1982.

[58] M. Dettenmaier and H. H. Kausch, "Light scattering of bisphenol-A polycarbonate in the amorphous state and at the beginning of thermal crystallization," *Colloid and Polymer Science*, vol. 259, no. 2, pp. 209–214, 1981.

[59] G. Floudas, A. Lappas, G. Fytas, and G. Meier, "Optical anisotropy and orientational dynamics of polycarbonate dilute solutions," *Macromolecules*, vol. 23, no. 6, pp. 1747–1753, 1990.

[60] Y. Aoki and J. O. Brittain, "Isothermal and nonisothermal dielectric relaxation studies on polycarbonate," *Journal of Polymer Science*, vol. 14, no. 7, pp. 1297–1304, 1976.

[61] H.-E. Carius, A. Schönhals, D. Guigner, T. Sterzynski, and W. Brostow, "Dielectric and mechanical relaxation in the blends of a polymer liquid crystal with polycarbonate," *Macromolecules*, vol. 29, no. 14, pp. 5017–5025, 1996.

[62] G. Locati and A. V. Tobolsky, *Studies of the Toughness of Polycarbonate of Bisphenol A in Light of Its secondary transition*, Princeton University, Princeton, NJ, USA, 1969.

[63] L. Delbreilh, E. Dargent, J. Grenet, J.-M. Saiter, A. Bernès, and C. Lacabanne, "Study of poly(bisphenol A carbonate) relaxation kinetics at the glass transition temperature," *European Polymer Journal*, vol. 43, no. 1, pp. 249–254, 2007.

[64] O. Mitxelena, J. Colmenero, and A. Alegría, "Effect of cold-drawing on the secondary dielectric relaxation of bisphenol-A polycarbonate," *Journal of Non-Crystalline Solids*, vol. 351, no. 33-36, pp. 2652–2656, 2005.

[65] A. Alegría, S. Arrese-Igor, O. Mitxelena, and J. Colmenero, "Dielectric secondary relaxation and phenylene ring dynamics in bisphenol-A polycarbonate," *Journal of Non-Crystalline Solids*, vol. 353, no. 47-51, pp. 4262–4266, 2007.

[66] S. A. Madbouly and J. U. Otaigbe, "Broadband dielectric spectroscopy of nanostructured maleated polypropylene/polycarbonate blends prepared by in situ polymerization and compatibilization," *Polymer*, vol. 48, no. 14, pp. 4097–4107, 2007.

[67] G. J. Pratt and M. J. A. Smith, "Dielectric response of commercial polycarbonate," *British Polymer Journal*, vol. 18, no. 2, pp. 105–111, 1985.

[68] H. W. Spiess, "Molecular dynamics of solid polymers as revealed by deuteron NMR," *Colloid & Polymer Science*, vol. 261, no. 3, pp. 193–209, 1983.

[69] M. L. Williams, R. F. Landel, and J. D. Ferry, "The temperature dependence of relaxation mechanisms in amorphous polymers and other glass-forming liquids," *Journal of the American Chemical Society*, vol. 77, no. 14, pp. 3701–3707, 1955.

[70] U. W. Gedde, *Polymer Physics*, Springer, 1995.

[71] E. Catsiff and A. V. Tobolsky, "Stress-relaxation of polyisobutylene in the transition region," *Journal of Colloid Science*, vol. 10, no. 4, pp. 375–392, 1955.

[72] J. M. Pochan, H. W. Gibson, M. F. Froix, and D. F. Hinman, "Dielectric relaxation studies of bisphenol A-diphenyl carbonate/lexan polycarbonate solid solutions," *Macromolecules*, vol. 11, no. 1, pp. 165–171, 1978.

[73] J. A. Campbell, A. A. Goodwin, and G. P. Simon, "Dielectric relaxation studies of miscible polycarbonate/polyester blends," *Polymer*, vol. 42, no. 10, pp. 4731–4741, 2001.

[74] B. J. Factor, F. I. Mopsik, and C. C. Han, "Dielectric behavior of a polycarbonate/polyester mixture upon transesterification," *Macromolecules*, vol. 29, no. 6, pp. 2318–2320, 1996.

[75] G. Katana, F. Kremer, E. W. Fischer, and R. Plaetschke, "Broadband dielectric study on binary blends of bisphenol-A and tetramethylbisphenol-A polycarbonate," *Macromolecules*, vol. 26, no. 12, pp. 3075–3080, 1993.

[76] C. Liu, C. Li, P. Chen, J. He, and Q. Fan, "Influence of long-chain branching on linear viscoelastic flow properties and dielectric relaxation of polycarbonates," *Polymer*, vol. 45, no. 8, pp. 2803–2812, 2004.

[77] A. S. Merenga, C. M. Papadakis, F. Kremer, J. Liu, and A. F. Yee, "Comparative broad-band dielectric study on poly(ester carbonate)s with 1,4-cyclohexylene linkages," *Macromolecules*, vol. 34, no. 1, pp. 76–81, 2001.

[78] E. El Shafee, G. R. Saad, and M. Zaki, "Calorimetric and dielectric study on poly(trimethylene terephthalate)/ polycarbonate blends," *Journal of Polymer Research*, vol. 15, no. 1, pp. 47–58, 2008.

[79] K. Mohomed, T. G. Gerasimov, F. Moussy, and J. P. Harmon, "A broad spectrum analysis of the dielectric properties of poly(2-hydroxyethyl methacrylate)," *Polymer*, vol. 46, no. 11, pp. 3847–3855, 2005.

[80] S. J. Havriliak and S. Havriliak Jr., *Dielectric and Mechanical Relaxation in Materials*, 1996.

[81] S. K. Emran, Y. Liu, G. R. Newkome, and J. P. Harmon, "Viscoelastic properties and phase behavior of 12-tert-butyl

ester dendrimer/poly(methyl methacrylate) blends," *Journal of Polymer Science B*, vol. 39, no. 12, pp. 1381–1393, 2001.

[82] P. Pissis and A. Kyritsis, "Electrical conductivity studies in hydrogels," *Solid State Ionics*, vol. 97, no. 1–4, pp. 105–113, 1997.

[83] M. G. Parthun and G. P. Johari, "Analyses for a dipolar relaxation in the featureless dielectric spectrum, and a comparison between the permittivity, modulus and impedance representations," *Journal of the Chemical Society, Faraday Transactions*, vol. 91, no. 2, pp. 329–335, 1995.

[84] J. H. Ambrus, C. T. Moynihan, and P. B. Macedo, "Conductivity relaxation in a concentrated aqueous electrolyte solution," *Journal of Physical Chemistry*, vol. 76, no. 22, pp. 3287–3295, 1972.

[85] A. K. Jonscher, "Dielectric relaxation in solids," *Journal of Physics D*, vol. 32, no. 14, pp. R57–R70, 1999.

[86] A. K. Jonscher, *Dielectric Relaxation in Solids*, 1983.

[87] R. A. Kalgaonkar and J. P. Jog, "Molecular dynamics of copolyester/clay nanocomposites as investigated by viscoelastic and dielectric analysis," *Journal of Polymer Science B*, vol. 46, no. 23, pp. 2539–2555, 2008.